Influence of pressure on the impedance of SnO_2 nanopowder

MUHAMMAD TARIQ SAEED CHANI[a,b*], SHER BAHADAR KHAN[a,b], ABDULLAH M. ASIRI[a,b], KH. S. KARIMOV[c,d], M. ABID[e], M. MEHRAN BASHIR[c], KALSOOM AKHTAR[f]

[a]*Center of Excellence for Advanced Materials Research (CEAMR), King Abdulaziz University, Jeddah21589, Saudi Arabia*

[b]*Chemistry Department, Faculty of Science, King Abdulaziz University, Jeddah 21589, Saudi Arabia*

[c]*GIK Institute of Engineering Sciences and Technology, Topi 23640, KPK, Pakistan*

[d]*Physical Technical Institute of Academy of Sciences, Dushanbe 734025, Tajikistan*

[e]*Interdisciplinary Research Center, COMSATS Institute of Information Technology, G.T. Road, Wah Cantt, Pakistan*

[f]*Division of Nano Sciences and Department of Chemistry, Ewha Womans University, Seoul, Korea*

In this paper, the influence of pressure on the impedance and resistance of SnO_2 nanopowder has been investigated. A transducer is fabricated for the direct measurement of impedance-pressure relationships on nanopowder. At initial conditions, the diameter and the height of nanopowder samples placed in the transducer are 10 mm and 3 mm, respectively. Under pressure of up to 8.15kN/m^2, the DC resistance and the impedance decrease on average up to 22% in the frequency range of 100 Hz to 200 kHz. This decrease in resistance and impedance may be regarded to the densification of samples and decrease in porosity under pressure. These impedance-pressure and resistance-pressure relationships are quasi-linear and it is also observed that the DC resistance increases with time and gets saturated within 5 minutes. This phenomenon is regarded to the effect of displacement currents of bound charges. The resistance-pressure relationship is simulated and the dependence of impedance phase (θ) on the frequency and pressure is also investigated.

(Received May 31, 2014; accepted January 21, 2015)

Keywords: Impedance, Tine oxide, Nanopowder, Pressure, Transducer

1. Introduction

Investigation of the effect of pressure on the properties of semiconductors is considered important for the understanding of basic properties of materials [1-3]. The study of conductivity and thermoelectric power of quasi-one and quasi-two dimensional organic semiconductors and conductor crystals shows that the conductivity of semiconductors increases and their thermoelectric coefficient decreases, while both the properties remain approximately constant in the conductors [4]. The influence of pressure on metal-insulator transitions in tetrathio-fulvalenium tetracyanoquinodimethane is investigated by Chu et al. [5]. On the other hand, the investigations of electric properties of materials, in particular of semiconductors can result in the fabrication of various kinds of sensors [6]. The pressure transducers are mostly used with resistance, capacitance, inductance, and piezoelectric sensors and also with devices such as diaphragm and bellows [6, 7]. The network of pressure sensors with organic transistors based on pentacene is fabricated and investigated under an applied pressure of 30kPa [8]. Unusual electromechanical effects (piezoelectricity and electrostriction) have been observed in Schottky junctions of organic semiconductors because of the presence of non-uniform spatial electric field distribution in the junction and softness of organic semiconductors. These effects can be potentially used for the fabrication of electromechanical transducers [9].

The CNTs based piezoresistors have been fabricated for use in mechanical sensors, such as strain gauges, pressure sensors and accelerometers [10-15]**.** The piezoresistance of CNTs on deformable thin-film silicon nitride membranes has been investigated by Nair et al. [13] and it is found that the gauge factors ($\Delta R/R\varepsilon$) are 400 and 850 for the semiconducting and small-gap semiconducting (SGS) tubes, respectively, whereas the maximum value of gauge factor in silicon is 200. By the investigation of small band-gap semiconducting (or quasi-metallic) nanotubes it is found that they exhibit piezoresistive gauge factor from 600 to 1000 under axial strains, which is much larger than in metallic nanotubes [10]. Xue et al. described the fabrication of single walled carbon nanotubes (SWNT) thin-film transistors on plastic substrates and their investigation shows that the resistance of the thin films containing 14 and 16 layers of SWNT decreases by 38.2% and 47.1%, respectively with increase in bending of the elastic substrate [15]. This decrease in resistance is more than 10 time higher than silicon. Li et al. studied the piezoresistive effect in the pristine CNTs films and found a gauge factor of 65 under 500 microstrains at room temperature, while the increase in temperature caused to increase the gauge facto [12]. The mechanical deformation-conductivity relationships of free-standing membranes of SWNTs are reported in ref. [11], which shows that the piezoresistive gauge factor of nanotubes is 2.3 to 2.5 times larger than that of the silicon substrate. The nano-electromechanical piezoresistance transducers

based on SWNTs have been investigated by Rittersma et al. and it is shown theoretically and experimentally that ballistically conducting SWNTs have nonlinear piezoresistive gauge factor up to 1500 (at applied strain 1%) [14].

In the majority of physical experiments for sensors the crystals, thin films and/or press-tablets are used. It would be reasonable to investigate the resistance-pressure relationships directly on powders. In this paper we have designed and fabricated transducer for the measurement of impedance of SnO_2 nanoparticles under pressure.

2. Experimental procedure

2.1 Synthesis of nanoparticles

For the synthesis of SnO_2, stannous chloride dihydrate (0.1 M) was dissolved in distilled water and the pH was raised above 10 by adding 0.5 M NaOH solution. The solution was then heated till the solvent was completely evaporated and a dried powder of SnO_2 was obtained, which was further grinded and used for detailed characterization and applications.

2.2 Characterization of nanoparticles

The morphology of synthesized SnO_2 is investigated by field emission scanning electron microscopy (JEOL FE-SEM, Japan), while the elemental analysis is carried out by using EDS (Oxford). The structural characterization is done by using FTIR spectroscopy (Perkin Elmer, spectrum 100). The optical properties are also analyzed by using UV-Vis spectrophotometer (UV-2960, LABOMED Inc.).

2.3 Fabrication of transducer and electrical characterization

For the investigation of impedance of SnO_2 nanopowder under pressure a transducer was fabricated, which is shown in Fig.1. The transducer consists of the following elements; cylinder-piston system, substrate, terminals and load. The cylinder is made of glass, while the piston and substrate are made of metal. Under the applied load, the powder squeezes between piston and the substrate. The diameter of the cylinder and the piston is 10 mm, while the initial height of powder in the cylinder is kept 3 mm. For the measurement of DC resistance and impedance (at 100 Hz, 1 kHz, 10 kHz, 100 kHz and 200 kHz) the MT 4090 LCR meter is used. The pressure of up to 8.15 kN m^{-2} can be attained by applying the variable load of 0.64 N (Fig. 1).

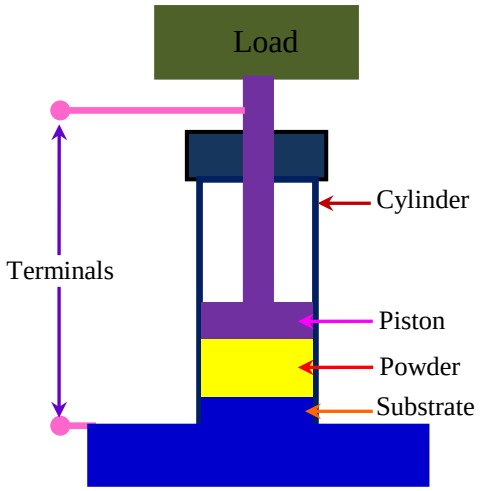

Fig. 1. Transducer for investigation of impedance of the powder under pressure.

3. Results and discussion

For the exploration of morphology and the measurement of size of synthesized SnO_2 nanoparticles, the FESEM was utilized. The morphology of SnO_2 is shown in Figs. 2a and 2b. It is evident from the FESEM images that the synthesized material is composed of aggregated nanoparticles having size of 20 nm on average. These nanoparticles having spherical shape were prepared in large quantity.

The composition of nanoparticles was evaluated by EDS spectrum, which is given in Fig.3. In the EDS spectrum of nanoparticles, the peaks at 0.5, 3.4 and 3.9 keV show the presence of only oxygen and Sn. The absence of any impurity peak confirms that synthesized nanomaterial is pure SnO_2.

The chemical structure of the SnO_2 nano-particles was also examined by FTIR analysis, which was recorded in the range of 400 cm^{-1} to 4000 cm^{-1} and shown in Fig. 4 (a). The intense bands observed at the 510 cm^{-1} are attributed to Sn–O bond. Supplementary peaks centered at 3270 and 1602 cm^{-1} are assigned to H_2O, while the peak at 1400 cm^{-1} is assigned to CO_2 absorbed from the environment [16].

The optical properties of metal oxides are generally realized by reflectivity and absorption measurements, which arise from the transition between electron and hole discrete or quantized electronic level [17, 18]. The optical properties of SnO_2 nano-particles are characterized by using a UV-Vis. spectrophotometer and the obtained spectrum is shown in Fig.4 (b). By using UV/visible absorption method, energy band gap of nanomaterials can also be find by analyzing their optical absorption. UV–vis absorption spectra exhibited an absorption peak at 295 nm and showed band gap energy equal to 3.8 eV, which is calculated by Tauc's formula. The relation between absorption coefficient (α) and the incident photon energy ($h\upsilon$) is given by the equation [19].

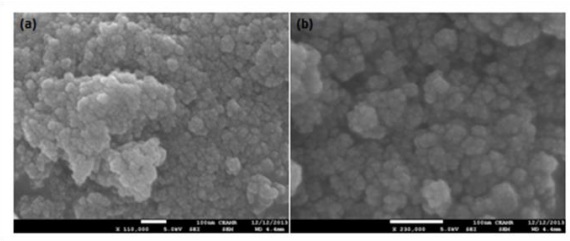

Fig. 2. Morphology of SnO_2 nanoparticles at lower (a) and higher (b) magnifications.

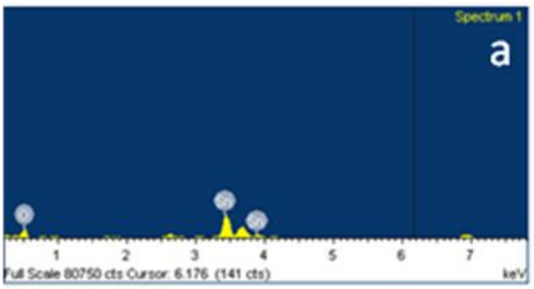

Element	Weight%	Atomic%
O K	48.54	87.50
Sn L	51.46	12.50
Totals	100.00	

b

Fig. 3. EDS spectrum (a) along with composition (b) of SnO_2 nanoparticles.

$$\alpha h\upsilon = A(h\upsilon - E_g)^n \quad (1)$$

where A is a constant, E_g is the band gap of the material and the exponent n depends on the type of transition, n = 1/2, 2, 3/2 and 3 corresponding to allowed direct, allowed indirect, forbidden direct and forbidden indirect, respectively. Taking n = 1/2, we have calculated the direct energy band gap from the $(\alpha h\upsilon)^{1/n}$ vs. $h\upsilon$ plots (Fig. 4 (c)).

Figs. 5(a) and 5(b) show the direct current (DC) resistance-pressure and impedance-pressure relationships at various frequencies for the SnO_2 nanoparticles, respectively. It was found that under pressure, the magnitudes of DC resistance and the impedance of the SnO2 samples decreased by 22% on average. This decrease in resistance and impedance can be explained by the densification of powder samples and reduction in their porosity due to the effect of pressure. As shown in the graphs (Fig. 5(a) and 5(b)) all relationships are quasi linear.

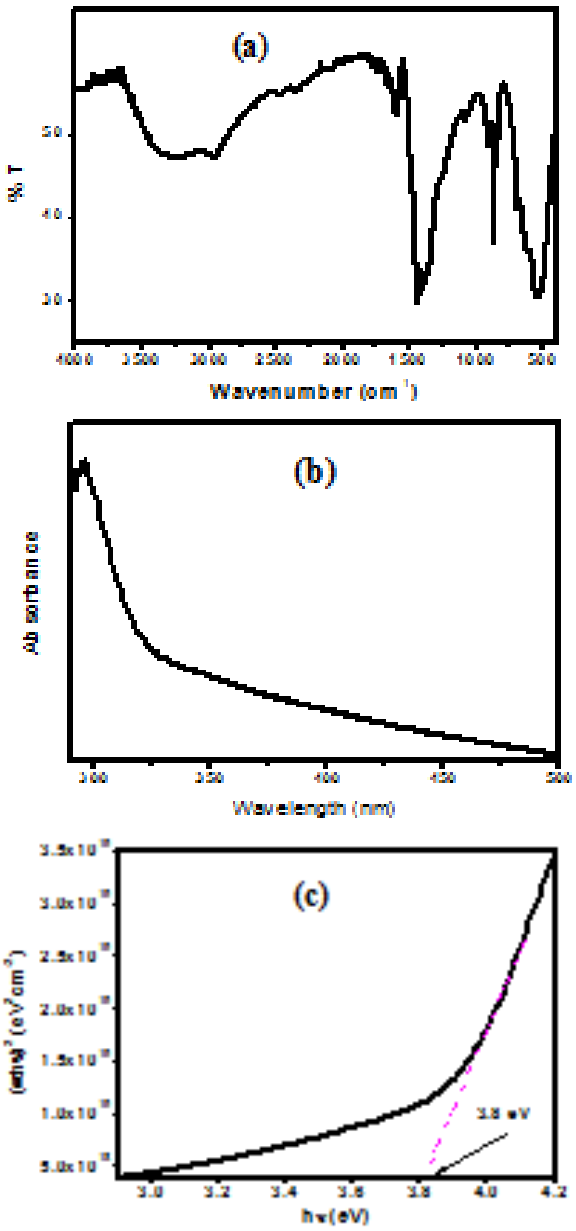

Fig. 4. FTIR (a) and UV-Vis (b & c) spectra of SnO_2 nanoparticles.

The transducer's resistance (R) can be represented by the following expression [20]:

$$R = {}^{d\rho}/_{A} = {}^{d}/_{\sigma A} \quad (2)$$

where d is the length or inter-electrode distance and A is the cross-section of the sample, ρ is resistivity ($\rho = 1/\sigma$, where σ is conductivity). By using Eq.2, the initial DC conductivity of the SnO2 nanoparticles is found 1.39 x 10^{-6} $\Omega^{-1}cm^{-1}$. The resistance-pressure relationship shown in Fig. 5 (a), may be due to the decrease in thickness (d) and accordingly porosity of the sample under applied pressure

or/and increase of the conductivity (σ) of the nanoparticles.

The Fig. 6 shows dependence of the DC resistance on the time under different applied pressures. It can be seen from the Fig. 6 that the DC resistances increase with time and gets saturated within 5 minutes. This phenomenon may be regarded to the effect of displacement currents of bound charges that is well known [21]. The increase in resistances with time under different pressures is on average on 36%.

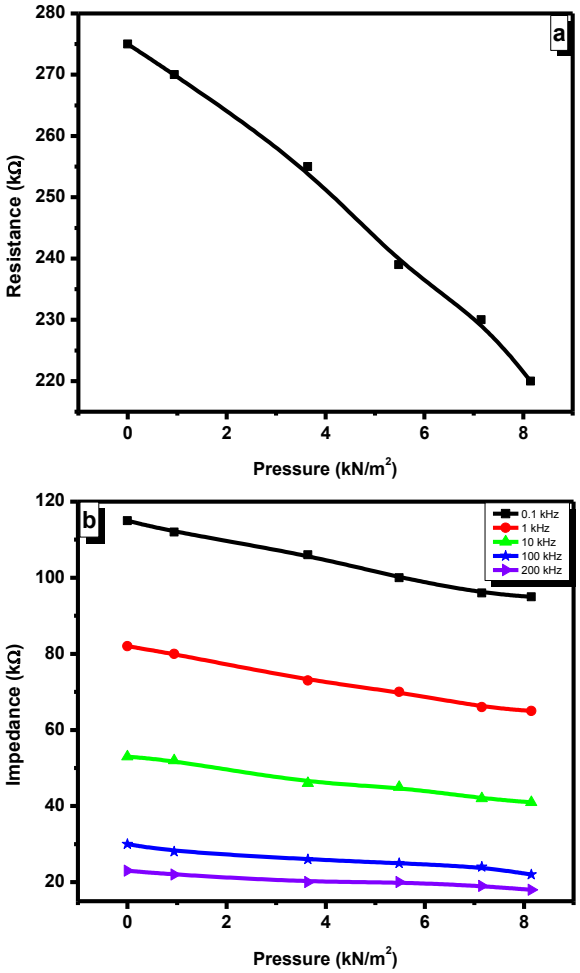

Fig. 5. DC resistance-pressure relationship (a) and impedance-pressure relationships (b) for the SnO_2 nanopowder at various frequencies.

The mechanism of conductivity in SnO2 nanoparticles can be considered as thermally assisted hopping transitions between spatially separated sites or particles that can be attributed to the Percolation Theory [22, 23]. The average conductivity (σ) according to the Percolation Theory can be calculated using following expression:

$$\sigma = {}^{1}/_{LZ} \tag{3}$$

where L is a characteristic length, depending on the concentration of the sites, Z is the resistance of the path with the lowest average resistance. With increase in pressure, firstly, L decreases and secondly Z. As a result, the conductivity increases and the resistance of the sample decrease accordingly, as observed experimentally (Fig. 5).

The simulation of resistance-pressure relationship can be done by using the following linear function [24]:

$$y = kx + b \tag{4}$$

For the resistance–pressure relationship the above function can be modified as follows:

$${}^{R}/_{R_o} = kp + b \tag{5}$$

where R and R_o are resistances of the sample under pressure (p) and at initial state and can be used for simulation of experimental data. The k is the fitting parameter and its value for resistance-pressure relation is -0.0245 m^2kN^{-1}. The Fig. 7 gives the comparison between the simulated and experimental results, which are observed in good agreement. All impedance-pressure relationships can also be simulated by using same approach.

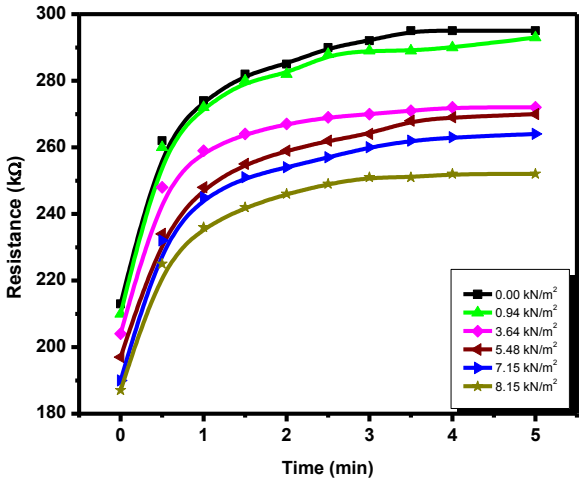

Fig. 6. DC resistance-time relationship for the SnO_2 nanopowder at different pressures.

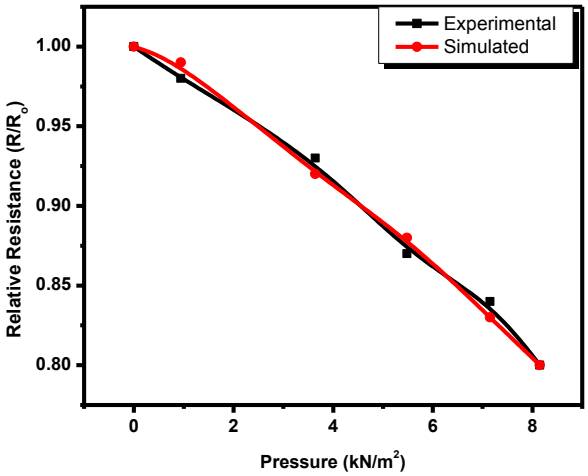

Fig. 7. Comparison of the experimental (1) and simulated (2) results.

The impedance (Z) of the sample is complex impedance and contains magnitude and phase ($Z=/Z/\angle\theta$). The Table 1 represents the values of the phases at initial state and largest pressure. It can be seen from the Table 1 that as frequency increases the phases increases at initial state and largest pressure as well. The dependency of the phase on the pressure varies with the variation of frequencies i.e. at frequencies of 100 Hz,1 kHz and 10 kHz the phase increases under applied pressure, but at 100 kHz and 200 kHz it decreases. It is considered that the equivalent electric circuit of the nanopowder samples can be represented by parallel connected resistor and capacitor (Fig. 8). The obtained experimental results and circuit analysis show that as the frequency (f) increases, the reactance ($1/2\pi fC$) decreases with respect to the resistance (R). With increase in pressure at lower frequencies, the reactance lowers relatively with respect to resistance, but at higher frequencies it increases relatively. The conduction current take place through nanoparticles, and the capacitance current–through porous as micro-capacitances, while the displacement currents of bound charges take place in the nanoparticles. The equivalent circuit presented in the Fig. 8 seems to be valid for the sample of nano powder and conductive micro units comprised of two neighboring nanoparticles.

Table 1. The values of the phases (θ) of the impedance at initial state and largest pressure (p) at different frequencies.

Pressure (KNm^{-2})	Frequency (kHz)					
	0.1	1	10	100	200	
0	-11.41	-15.2	-20.80	-30.43	-36.30	Phase θ (deg)
8.15	-14.22	-18.01	-21.50	-28.27	-32.70	

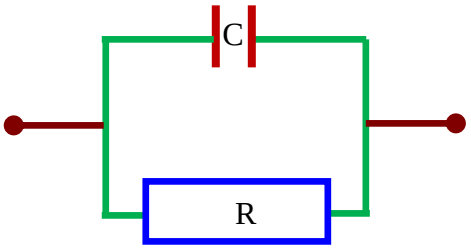

Fig. 8. The equivalent electric circuit of the nanopowder samples.

4. Conclusion

A transducer for the direct measurement of the influence of pressure on the impedance of powder was fabricated. The transducer allows to measure impedance of different kinds of powders without any preliminary processing. In this study we investigated the SnO2 nanopowder; under pressure the DC resistance and impedance at 100 Hz, 1 kHz, 10 kHz, 100 kHz and 200 kHz were decreased by 22% on average. It was also observed that the DC resistance increases with time and gets saturated within 5 minutes. As impedance can be represented as a complex number, the dependence of the phase (θ) on frequency and pressure was also investigated. The investigated nanopowder samples have been represented as parallel connected capacitor and resistor, where conduction takes place through capacitors (i.e. micro-pores) and resistors (i.e. nanoparticles) as well. The changes of frequency and/or pressure resulted in changes of the "resistors" and "capacitors".

Acknowledgment

This paper was funded by King Abdulaziz University, under grant No. (D-004/431). The authors, therefore, acknowledge the technical and financial support of KAU.

References

[1] M. Brahmia, B. Bennecer, A. Hamidani, J. Phys. Chem. Solids **74**, 1336 (2013).
[2] M. B. Kanoun, S. G. Said, A. E. Merad, G. Merad, J. Cibert, H. Aourag, Semicond. Sci. Technol. **19**, 1220 (2004).
[3] F. S. Saoud, J. C. Plenet, M. Henini, Physica B **407**, 1008 (2012).
[4] K. S. Karimov, D.Sc Thesis, Department of Heat Physics, Academy of Sciences, Tashkent, Uzbekistan, (1994).
[5] C. W. Chu, J. M. E. Harper, T. H. Geballe, R. L. Greene, Phys. Rev. Lett. **31**, 1491(1973).
[6] J. W. Dally, W. Riley, K. G. McConnell, Instrumentation for engineering measurements, John Wiley and Sons Inc., New York, 1993.
[7] C. D. Simpson, Industrial electronics, Prentice Hall, Inc., Englewood Cliffs, New Jersey, 1996.
[8] T. Someya, Y. Kato, T. Sekitani, S. Iba, Y. Noguchi, Y. Murase, H. Kawaguchi, T. Sakurai, Proceedings of the National Academy of Sciences, USA **102**, 12321 (2005).
[9] G. Dennler, C. Lungenschmied, N. S. Sariciftci, R. Schwödiauer, S. Bauer, H. Reiss, Appl. Phys. Lett. **87**, 163501 (2005).
[10] J. Cao, Q. Wang, H. Dai, Phys. Rev. Lett. **90**, 157601 (2003).
[11] G. Epifanov, Y. A. Moma, Solid state electronics, V Shkola, Moscow, 1986.
[12] Y. Li, W. Wang, K. Liao, C. Hu, Z. Huang, Q. Feng,

Chin. Sci. Bull. **48**, 125 (2003).
[13] M. T. S. Nair, L. Guerrero, O. L. Arenas, P. K. Nair, Appl. Surf. Sci. **150**, 143 (1999).
[14] Z. Rittersma, Sens. Actuators, A **96**, 196 (2002).
[15] W. Xue, T. Cui, 14th International Conference on Solid-State Sensors, Actuators and Microsystems, IEEE, Lyon, France, 1047, 2007.
[16] S. B. Khan, M. T. S. Chani, K. S. Karimov, A. M. Asiri, B. Mehran, T. Rana, Talanta **120**, 443 (2014).
[17] B. J. Scott, G. Wirnsberger, G. D. Stucky, Chem. Mater. **13**, 3140 (2001).
[18] A. D. Yoffe, Adv. Phys. **50**, 1 (2001).
[19] A. M. Asiri, M. M. Rehman, S. B. Khan, A. G. Al-Sehemi, S. A. Al-Sayari, M. S. Al-Assiri, Nanoscale Res. Lett. **8**, 380 (2013).
[20] M. A. Omar, Elementary Solid State Physics: Principles and Applications, Pearson Education (Singapore) Pt. Ltd., Indian branch, Delhi, India, 2002.
[21] D. V. Sivukhin, Physics,Electricity, Nauka, Moscow, 1977.
[22] H. Bottger, V. V. Bryksin, VCH, Deerfield Beach, FL 1985
[23] C. Brabec, J. P. a. N. S. V. Dyakonov, Organic Photovoltaics: Concepts and Realization, Springer-Verlag, Berlin Heidelberg, 2003.
[24] A. Croft, T. Croft, R. Davison, and M. Hargreaves, Engineering mathematics: a modern foundation for electronic, electrical, and control engineers, Addison-Wesley, 1992.

*Corresponding author: tariqchani1@gmail.com